Myocardial CT Perfusion Imaging and SPECT for the Diagnosis of Coronary Artery Disease: A Head-to-Head Comparison from the CORE320 Multicenter Diagnostic Performance Study[1]

Richard T. George, MD
Vishal C. Mehra, MD, PhD
Marcus Y. Chen, MD
Kakuya Kitagawa, MD, PhD
Armin Arbab-Zadeh, MD, PhD
Julie M. Miller, MD
Matthew B. Matheson, MS
Andrea L. Vavere, MS
Klaus F. Kofoed, MD
Carlos E. Rochitte, MD, PhD
Marc Dewey, MD, PhD
Tan S. Yaw, MD
Hiroyuki Niinuma, MD, PhD
Winfried Brenner, MD, PhD
Christopher Cox, PhD
Melvin E. Clouse, MD
João A. C. Lima, MD
Marcelo Di Carli, MD

[1] From the School of Medicine, Johns Hopkins University, 600 N Wolfe St, Blalock 524D2, Baltimore, MD 21287 (R.T.G., V.C.M., A.A.Z., J.M.M., A.L.V., J.A.C.L.); Department of Epidemiology, Bloomberg School of Public Health, Baltimore, Md (M.B.M., C.C.); Department of Nuclear Medicine and Cardiovascular Imaging, Brigham and Women's Hospital, Boston, Mass (M.D.C.); Department of Cardiology, Heart Institute (InCor), University of São Paulo Medical School, São Paulo, Brazil (C.E.R.); National Heart Lung and Blood Institute, National Institutes of Health, Bethesda, Md (V.C.M., M.Y.C.); Department of Radiology, Iwate Medical University, Morioka, Japan (H.N.); Department of Radiology, St. Luke's International Hospital, Tokyo, Japan (H.N.); Department of Radiology, Mie University Hospital, Tsu, Japan (K.K.); Department of Radiology, Beth Israel Deaconess Medical Center, Harvard University, Boston, MA (M.E.C.); Department of Radiology, Rigshospitalet, University of Copenhagen, Copenhagen, Denmark (K.F.K.); Department of Cardiology, National Heart Center, Singapore, Singapore (T.S.Y.); and Departments of Radiology (M.D.C.) and Nuclear Medicine (W.B.), Charité–University Medicine Berlin, Berlin, Germany. Received April 4, 2014; revision requested April 18; revision received April 28; accepted May 5; final version accepted May 9. Supported in part by the Intramural Research Program of the NIH, National Heart, Lung and Blood Institute. **Address correspondence to** R.T.G. (e-mail: *rgeorge3@jhmi.edu*).

Purpose: To compare the diagnostic performance of myocardial computed tomographic (CT) perfusion imaging and single photon emission computed tomography (SPECT) perfusion imaging in the diagnosis of anatomically significant coronary artery disease (CAD) as depicted at invasive coronary angiography.

Materials and Methods: This study was approved by the institutional review board. Written informed consent was obtained from all patients. Sixteen centers enrolled 381 patients from November 2009 to July 2011. Patients underwent rest and adenosine stress CT perfusion imaging and rest and either exercise or pharmacologic stress SPECT before and within 60 days of coronary angiography. Images from CT perfusion imaging, SPECT, and coronary angiography were interpreted at blinded, independent core laboratories. The primary diagnostic parameter was the area under the receiver operating characteristic curve (A_z). Sensitivity and specificity were calculated with use of prespecified cutoffs. The reference standard was a stenosis of at least 50% at coronary angiography as determined with quantitative methods.

Results: CAD was diagnosed in 229 of the 381 patients (60%). The per-patient sensitivity and specificity for the diagnosis of CAD (stenosis ≥50%) were 88% (202 of 229 patients) and 55% (83 of 152 patients), respectively, for CT perfusion imaging and 62% (143 of 229 patients) and 67% (102 of 152 patients) for SPECT, with A_z values of 0.78 (95% confidence interval: 0.74, 0.82) and 0.69 (95% confidence interval: 0.64, 0.74) ($P = .001$). The sensitivity of CT perfusion imaging for single- and multivessel CAD was higher than that of SPECT, with sensitivities for left main, three-vessel, two-vessel, and one-vessel disease of 92%, 92%, 89%, and 83%, respectively, for CT perfusion imaging and 75%, 79%, 68%, and 41%, respectively, for SPECT.

Conclusion: The overall performance of myocardial CT perfusion imaging in the diagnosis of anatomic CAD (stenosis ≥50%), as demonstrated with the A_z, was higher than that of SPECT and was driven in part by the higher sensitivity for left main and multivessel disease.

Coronary computed tomographic (CT) angiography is capable of depicting coronary artery disease (CAD) from its early to later stages and can help define percentage diameter stenosis, coronary atherosclerotic plaque characteristics, and burden in a noninvasive manner. However, when there is a need to evaluate the hemodynamic significance of CAD, physiologic tests such as electrocardiographic stress testing, radionuclide perfusion imaging, and stress echocardiography have been the most commonly used noninvasive diagnostic strategies.

Advances in Knowledge

- Myocardial CT perfusion imaging demonstrates higher overall diagnostic performance compared with SPECT myocardial perfusion imaging for the detection of anatomic stenosis (defined as ≥50% diameter stenosis at quantitative coronary angiography), with area under the receiver operating characteristic curve of 0.78 (95% confidence interval: 0.74, 0.82) for CT perfusion imaging and 0.69 (95% confidence interval: 0.64, 0.74) for SPECT (P = .001).
- In the detection of stenosis of at least 50% with use of prespecified cutoffs for both SPECT and CT perfusion imaging, the sensitivity of CT perfusion imaging is higher than that of SPECT (88% vs 62%, $P < .001$); the specificity of CT perfusion imaging is lower than that of SPECT (55% vs 67%, P = .02).
- The higher sensitivity of CT perfusion imaging is driven by a higher sensitivity for single- and multivessel coronary artery disease (CAD) compared with SPECT, with sensitivities for left main, three-vessel, two-vessel, and one-vessel disease of 92%, 92%, 89%, and 83%, respectively, for CT perfusion imaging and 75%, 79%, 68%, and 41%, respectively, for SPECT.

More recently, technical advances in cardiac CT have made feasible the development of myocardial CT perfusion imaging. Single-center studies have established that myocardial CT perfusion imaging can help accurately diagnose CAD compared with various reference standards including single photon emission computed tomography (SPECT), invasive coronary angiography, magnetic resonance (MR) imaging, and fractional flow reserve (1–4). Recently, the combination of coronary CT angiography and myocardial CT perfusion imaging was validated in the multicenter diagnostic accuracy study Combined Coronary Atherosclerosis and Myocardial Perfusion Evaluation Using 320–Detector Row CT (CORE320) by using a hybrid anatomic and physiologic reference standard (5). This prospective multicenter study also provides the opportunity to independently validate the diagnostic performance of CT perfusion imaging and SPECT in the diagnosis of anatomic CAD.

Clinical validation of noninvasive tests for the diagnosis of CAD most often begins with a comparison with the invasive standard of reference used to define CAD, namely invasive coronary angiography (6–8), by using quantitative coronary angiography analysis and stenosis of at least 50% as the definition of abnormal. The 50% threshold has been selected as a result of studies demonstrating decreases in hyperemic myocardial blood flow as a stenosis reaches the 50% threshold (9,10), and this quantitative threshold correlates well with a visually determined stenosis of 70% severity (11).

In this prespecified, secondary analysis of the CORE320 study, the primary aim was to compare the diagnostic performance of CT perfusion imaging and SPECT perfusion imaging in the diagnosis of anatomic CAD (≥50% stenosis) as depicted at invasive coronary angiography.

Implications for Patient Care

- This study demonstrates that CT perfusion imaging is a viable alternative to SPECT myocardial perfusion imaging for the detection of CAD.
- CT perfusion imaging maintains sensitivity for detecting coronary disease in patients with left main and multivessel disease.

Materials and Methods

Patient Population

The CORE320 study is a prospective, multicenter, international, diagnostic accuracy study that was performed at 16 centers in eight countries (*www.clinicaltrials.gov*, NCT00934037). The CORE320 study design (12,13) and primary results (5) have been previously described. The study's sponsor, Toshiba Medical Systems, was not involved in any stage of the study design, data acquisition, data analysis, or manuscript preparation. The study's investigators

Published online before print
10.1148/radiol.14140806 **Content code:** CA

Radiology 2014; 272:407–416

Abbreviations:
A_z = area under the receiver operating characteristic curve
CAD = coronary artery disease
CI = confidence interval
CORE320 = Combined Coronary Atherosclerosis and Myocardial Perfusion Evaluation Using 320–Detector Row CT
NPV = negative predictive value
PPV = positive predictive value
SSS = summed stress score

Author contributions:
Guarantors of integrity of entire study, R.T.G., H.N., J.A.C.L.; study concepts/study design or data acquisition or data analysis/interpretation, all authors; manuscript drafting or manuscript revision for important intellectual content, all authors; manuscript final version approval, all authors; agrees to ensure any questions related to the work are appropriately resolved, all authors; literature research, R.T.G., V.C.M., A.A.Z., J.M.M., C.E.R., H.N., W.B., M.E.C., J.A.C.L.; clinical studies, R.T.G., V.C.M., M.Y.C., K.K., A.A.Z., J.M.M., K.F.K., C.E.R., M.D., T.S.Y., H.N., W.B., M.E.C., M.D.C.; statistical analysis, V.C.M., M.B.M., A.L.V., H.N., W.B., C.C.; and manuscript editing, R.T.G., V.C.M., M.Y.C., A.A.Z., J.M.M., A.L.V., K.F.K., C.E.R., M.D., H.N., W.B., C.C., M.E.C., J.A.C.L., M.D.C.

Funding:
This research was supported in part by the Intramural Research Program of the National Institutes of Health, National Heart, Lung, and Blood Institute (grant ZIA HL006138-03).

Conflicts of interest are listed at the end of this article.

had full control of the data. In addition, this research was supported in part by the Intramural Research Program of the National Institutes of Health, National Heart, Lung, and Blood Institute.

In brief, the study included men and women aged 45–85 years with a clinical referral for invasive coronary angiography. Subjects were enrolled from November 2009 to July 2011. The protocol was approved by local and central institutional review boards, and all patients provided informed consent before participation. Exclusion criteria included the following: allergy to iodinated contrast material, serum creatinine level greater than 1.5 mg/dL or calculated creatinine clearance of less than 60 mL/min, atrial fibrillation, second- or third-degree atrioventricular block, previous cardiac surgery, recent coronary intervention, evidence of an acute coronary syndrome with a thrombolysis in myocardial infarction score of at least 5 or elevated cardiac enzymes in the past 72 hours, and a body mass index greater than 40 kg/m^2. A complete list of the exclusion criteria is given in references 13 and 14.

All subjects underwent resting coronary CT angiography, an adenosine stress myocardial CT perfusion study, and either an exercise or pharmacologic SPECT myocardial perfusion imaging study within 60 days of coronary angiography.

Rest CT Angiography and Adenosine Stress Myocardial CT Perfusion Imaging and Analysis

The methods used for rest CT angiography, CT perfusion imaging, and adenosine stress myocardial CT perfusion imaging have been previously described (12). All imaging was performed with a 320–detector row CT unit (Aquilion One; Toshiba Medical Systems, Otawara, Japan), and all sites underwent site qualification (13). In brief, patient preparation included 75–150 mg of oral metoprolol and intravenous metoprolol if the baseline heart rate was more than 60 beats per minute. With use of prospective electrocardiographic triggering, 0.4 mg of a fast-acting sublingual nitrate was administered and rest CT perfusion imaging performed with 50–70 mL of iodinated contrast material (iopamidol, 370 mg of iodine per milliliter). Twenty minutes later, adenosine (0.14 mg/kg/min) was infused and stress CT perfusion imaging was performed with 50–70 mL of iopamidol and prospective electrocardiographic triggering (12).

Coronary CT angiograms and myocardial CT perfusion images were reconstructed and transferred to two separate, independent, and blinded core laboratories (12). For the purposes of this secondary analysis, CT angiography data were not included. It is important to emphasize that the CT perfusion core laboratory (Johns Hopkins University) was blinded to the CT angiography data by reconstructing images with a myocardial CT perfusion kernel, setting the workstation to a window width of 300 HU and window level of 150 HU and locking the workstation at a section thickness of at least 3 mm. By doing so, the CT angiogram is not interpretable for percentage stenosis. CT perfusion images were visually interpreted by two independent and experienced observers (R.T.G. and V.C.M., with 7 years and 1 year of experience in CT), with differences resolved by consensus. With use of a previously described 13-segment myocardial model (12,14), rest and stress myocardial segments were scored as follows: 0 = normal, 1 = mild, 2 = moderate, and 3 = severe perfusion defect. A summed stress score (SSS) was calculated as the sum of all segmental scores. A 13-segment myocardial model was selected to simplify the registration of coronary anatomy and myocardial segments and to reduce variability between the modalities.

SPECT Myocardial Perfusion Imaging Acquisition and Analysis

All SPECT cameras underwent a qualification process that was monitored by the SPECT core laboratory. The procedures of the independent SPECT core laboratory have been previously described (12–14). SPECT was performed by using technetium 99m–labeled imaging agents, with approximately 300 MBq used for rest studies and 925 MBq used for stress studies. Studies were performed without attenuation correction available. Exercise or pharmacologic stress testing was performed with use of standardized protocols (15). SPECT images were transferred to an independent core laboratory at Brigham and Women's Hospital and interpreted visually by two independent and experienced observers (M.D.C., with 23 years of experience, and a nonauthor with 13 years of experience; both readers were board certified in nuclear medicine or nuclear cardiology), with differences resolved by consensus between the two readers using parallel methods to those used by the CT perfusion core laboratory. The SSS was calculated as described earlier. In the analysis, artifacts did not contribute to the SSS; therefore, an SSS of at least 1 was indicative of an abnormal SPECT study.

Coronary Angiography Acquisition and Analysis

Coronary angiography was performed before and within 60 days of CT and SPECT in a CORE320-qualified laboratory. Images were transferred to the independent coronary angiography core laboratory at Johns Hopkins University. The coronary artery tree was segmented by using standard software (CAAS; PIE Medical Imaging, Maastricht, the Netherlands), and all coronary segments of at least 2 mm were analyzed for percentage diameter stenosis by using quantitative coronary angiography methods as previously described (16).

Statistical Analysis

All data were analyzed in the statistical core laboratory at the Bloomberg School of Public Health. In the primary analysis, we estimated the diagnostic performance of CT perfusion and SPECT myocardial perfusion imaging in the diagnosis of a stenosis of at least 50% at quantitative coronary angiography on a per-patient and per-vessel basis.

The primary analysis was based on the area under the receiver operating characteristic curve (A_z) (empirical form). For the standard of reference, each patient or vessel was classified as having normal findings or CAD, which

was defined as a stenosis of at least 50% at quantitative coronary angiography. The receiver operating characteristic curve was based on a logistic regression analysis, with CT perfusion imaging or SPECT as the predictor variables. Sensitivity, specificity, and predictive values were calculated for SPECT and CT perfusion imaging by using a prespecified SSS threshold of at least 1 for SPECT and at least 2 for CT perfusion imaging. Secondary per-vessel analyses were adjusted for the effects of within-patient clustering by using the bootstrap method with resampling at the patient level. Posthoc analyses included the use of a stenosis of at least 70% at quantitative coronary angiography and a subgroup analysis of only the subjects who underwent pharmacologic stress SPECT myocardial perfusion imaging.

All data are reported with 95% confidence intervals (CIs). *P* values were calculated with the bootstrap method for A_z values and with the generalized estimating equation for point statistics. $P < .05$ was indicative of a significant difference.

A_z analysis was performed with software (STATA 11, with use of the roctab and roccomp commands, as well as the bootstrap method, for the all-vessel comparison and CIs); graphics were created in S-plus 8.0, and descriptive statistics and the point statistics (and comparisons thereof) were performed in SAS 9.1.

Results

A total of 436 eligible patients were enrolled in the study from November 2009 to July 2011; 55 subjects were excluded because all imaging procedures were not completed ($n = 29$), technical failure of SPECT ($n = 12$), technical failure of or incomplete imaging with CT ($n = 13$), or technical failure of coronary angiography ($n = 1$) (5). Of the 381 subjects with complete imaging data sets included in this analysis, 257 underwent pharmacologic SPECT and 124 underwent exercise SPECT (69% [86 of 124 subjects] reached 85% maximum predicted heart rate and 83% [103 or 124 subjects] reached 80% maximum predicted heart rate). Baseline characteristics are shown in Table 1. The median effective

Table 1

Baseline Characteristics

Characteristic	Value
Age (y)	
All patients	
Median*	62 (41–82)
Interquartile range	56–68
Men	
Median*	63 (41–82)†
Interquartile range	56–69
Women	
Median*	61 (48–82)
Interquartile range	55–66
Male sex	252 (66)
Ethnicity	
Hispanic	32 (8)
Non-Hispanic	326 (86)
Other	23 (6)
Race	
White	213 (56)
Black	40 (10)
Asian	123 (32)
Other	5 (1)
Body mass index (kg/m²)	
Median*	27 (16–51)
Interquartile range	24–30
Hypertension	297 (78)
Diabetes	131 (34)
Dyslipidemia	254 (68)
Previous myocardial infarction	103 (27)
Smoking	
Current	64 (18)
Past	133 (37)
Never	167 (46)
Family history of CAD	162 (45)
Previous percutaneous coronary intervention	113 (30)
Medications	
Angiotensin-converting enzyme inhibitors/ angiotensin receptor blockers	146 (38)
β-blocker	173 (45)
Salicylates	172 (45)
Nitrates	47 (12)
Other antihypertensive medications	64 (17)
Angina in the 30 d before enrollment (Canadian class)	
NA‡	83 (22)
0	61 (16)
1	110 (30)
2	99 (27)
3	14 (4)
4	4 (1)

Table 1 (continues)

Table 1 (continued)

Baseline Characteristics

Characteristic	Value
Unstable angina in the 30 d before enrollment	2 (1)
Previous stress testing in the 3 mo before enrollment	
Electrocardiography only	16 (4)
Echocardiography	8 (2)
Results of stress testing	
Positive	12 (52)
Negative/equivocal	11 (48)
Calcium score§	
Median*	162 (0–4401)
Interquartile range	9–530
Mean ± standard deviation	423 ± 668
Rest CT perfusion imaging	
Contrast material dose	
50 mL	51 (13)
60 mL	310 (81)
70 mL	2 (1)
β-blocker (oral)	
75 mg	129 (34)
150 mg	190 (50)
None	62 (16)
Nitroglycerin during imaging	329 (86)
Heart rate during imaging	
Median*	53 (35–121)
Interquartile range	49–59
Radiation exposure (mSv)	
Median*	3.16 (2.12–13.68)
Interquartile range	2.82–3.59
Stress CT perfusion imaging	
Contrast material dose	
50 mL	52 (14)
60 mL	1 (0)
70 mL	308 (81)
Heart rate during imaging	
Median*	69 (33–109)
Interquartile range	60–78
Radiation exposure (mSv)	
Median*	5.31 (2.36–8.60)
Interquartile range	3.83–6.02
SPECT	
SPECT type	
Pharmacologic	257 (67)
Exercise	124 (33)
Clinically driven	157 (41)
Research driven	224 (59)
Radiation exposure (mSv)	
Median*	9.75 (1.93–15.91)
Interquartile range	9.10–12.95

Table 1 (continues)

Table 1 (continued)

Baseline Characteristics

Characteristic	Value
Invasive coronary angiography	
Nitroglycerin during angiography	352 (92)
Contrast material dose (mL)	
Median*	100 (25–450)
Interquartile range	75–131
Radiation exposure (mSv)	
Median*	11.97 (0.79–70.98)
Interquartile range	7.60–17.80

Note.—Except where indicated, data are numbers of patients, with percentages in parentheses.

* Numbers in parentheses are ranges.

† $P = .036$.

‡ NA = not applicable.

§ Determined with the Agatston method.

Figure 1

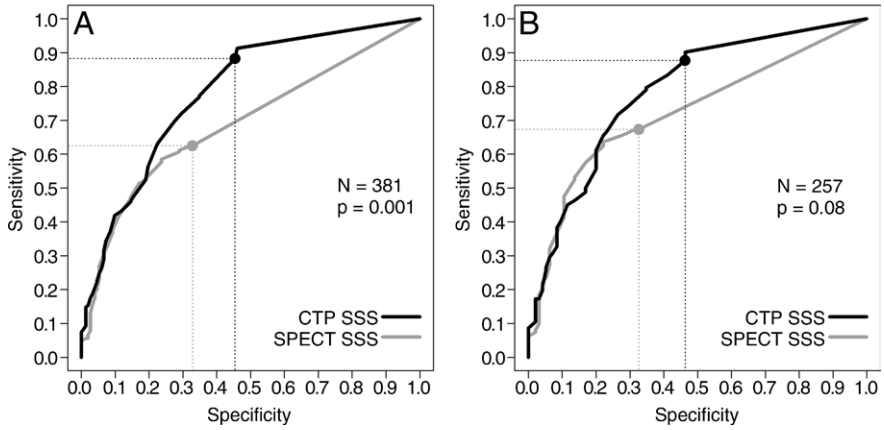

Figure 1: Receiver operating characteristic curves for myocardial CT perfusion imaging (*CTP*) and SPECT in, *A*, all patients and, *B*, only the patients who underwent pharmacologic stress SPECT.

radiation doses for CT perfusion imaging, SPECT, and coronary angiography were previously reported and are listed in Table 1 (5).

Diagnostic Performance of Myocardial CT Perfusion Imaging and SPECT

Per-patient analysis.—In the prespecified per-patient analysis with use of a stenosis of at least 50% at coronary angiography as the standard of reference, the A_z for CT perfusion imaging was 0.78 (95% CI: 0.74, 0.82) when all patients were included (Fig 1). Figure 2 demonstrates a representative case from the study. This was significantly higher than that of SPECT, which had an A_z of 0.69 (95% CI: 0.64, 0.74) ($P = .001$) (Table 2). This difference was consistent with a higher sensitivity for CT perfusion imaging and a higher specificity for SPECT. The positive predictive value (PPV) was similar for both CT perfusion imaging and SPECT, but the negative predictive value (NPV) was higher for CT perfusion imaging.

At posthoc subgroup analysis limited to patients who underwent pharmacologic SPECT ($n = 257$), the A_z for CT perfusion imaging (0.78; 95% CI: 0.73, 0.83) was higher than that for SPECT (0.72; 95% CI: 0.66, 0.78), but with borderline significance ($P = .08$). Sensitivity ($P < .001$) and NPV ($P = .003$) remained higher for CT perfusion imaging; there was no significant difference between CT perfusion imaging and SPECT with regard to specificity and PPV.

At posthoc analysis, we examined the A_z of CT perfusion imaging and SPECT in the prediction of a stenosis of at least 70%. The A_z for CT perfusion imaging was 0.78 (95% CI: 0.73, 0.82), and the sensitivity, specificity, PPV, and NPV were 92% (95% CI: 87, 96; 160 of 174 patients), 46% (95% CI: 39, 53; 96 of 207 patients), 59% (95% CI: 53, 65; 160 of 271 patients), and 87% (95% CI: 80, 93; 96 of 110 patients), respectively. These data were not significantly different from those of SPECT ($P = .36$), which had an A_z of 0.75 (95% CI: 0.71, 0.80) and a sensitivity, specificity, PPV, and NPV of 72% (95% CI: 65, 78; 125 of 174 patients), 67% (95% CI: 60, 74; 139 of 207 patients), 65% (95% CI: 58, 71; 125 of 193 patients), and 74% (95% CI: 67, 80; 139 of 188 patients), respectively. Sensitivity was higher for CT perfusion imaging ($P < .001$) and specificity was higher for SPECT ($P < .001$), with no significant difference in PPV. NPV was higher for CT perfusion imaging ($P = .002$).

Per-vessel analysis.—In the per-vessel analysis, the A_z of CT perfusion imaging (0.74; 95% CI: 0.71, 0.78) was higher than that of SPECT (0.69; 95% CI: 0.66, 0.72) for the diagnosis of a stenosis of at least 50% when considering all vessels ($P = .008$, Table 3). For individual vessels, the A_z was significantly higher for the left anterior descending artery ($P = .02$), was borderline higher for the left circumflex artery ($P = .05$), and showed no significant difference for the right coronary artery ($P = .43$).

In the posthoc analysis using a quantitative coronary angiography–defined stenosis of at least 70%, there were no significant differences between the A_z for CT perfusion imaging (0.73; 95% CI: 0.70, 0.77) and SPECT (0.75; 95% CI: 0.71, 0.78) ($P = .48$) when considering all vessels as well as individual vessels.

Sensitivity for Left Main, Multivessel, and Single-Vessel Disease

Left main, three-vessel, two-vessel, and one-vessel disease was present in 3.1% (12 of 381 patients), 17.3% (66 of 381 patients), 19.7% (75 of 381 patients), and 19.9% (76 of 381 patients) of patients, respectively. The sensitivity of CT perfusion imaging was higher than that of SPECT for all disease categories (Table 4).

Discussion

This study demonstrated that the A_z for myocardial CT perfusion imaging was

Figure 2

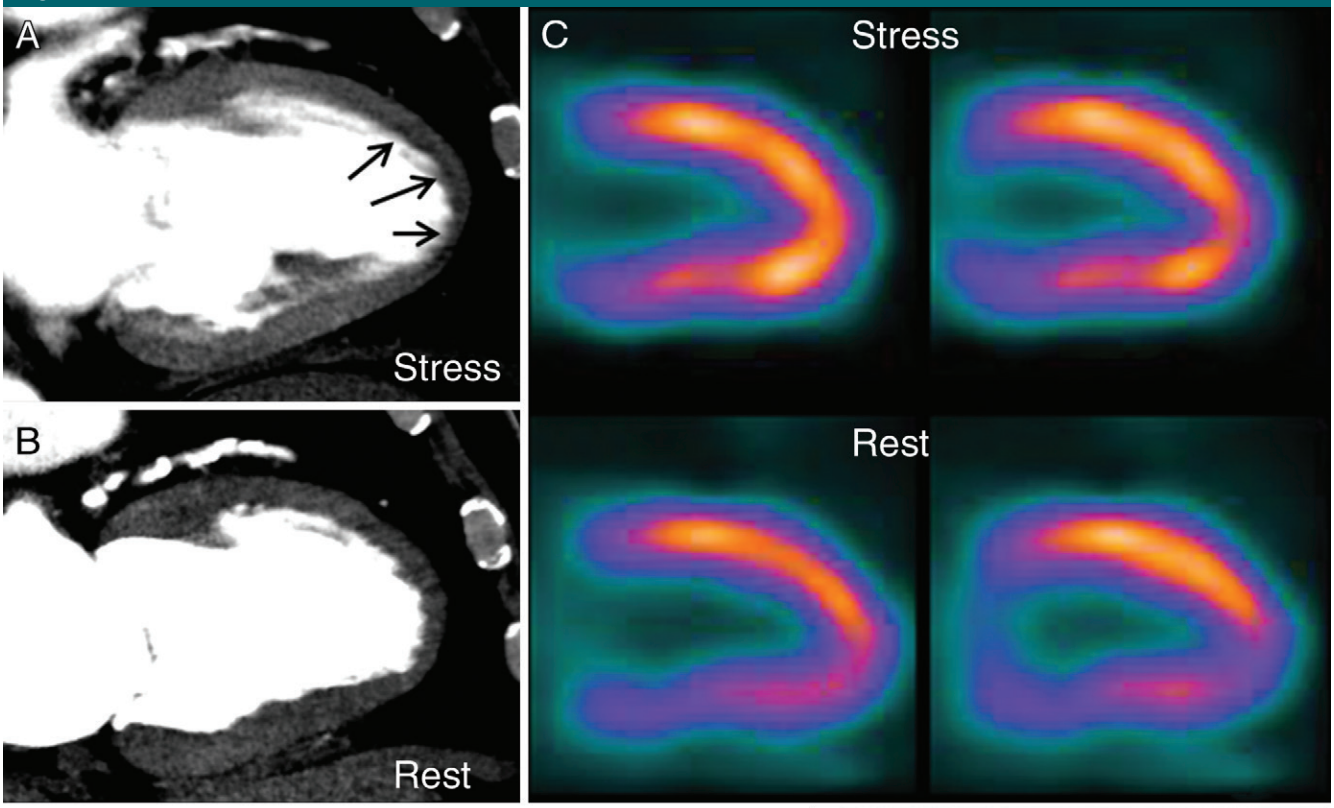

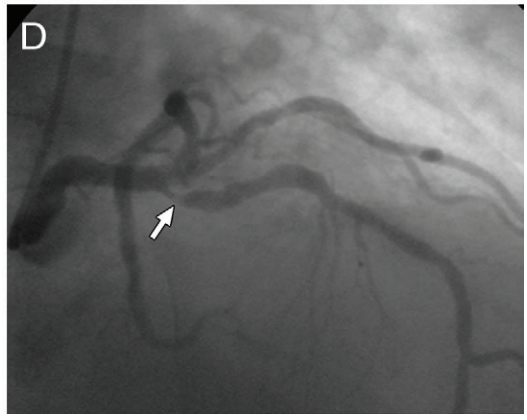

Figure 2: Images in 80-year-old man with chest pain. *A*, Myocardial CT perfusion image at stress demonstrates subendocardial perfusion defect in anteroapical and apical walls (arrows). *B*, Myocardial CT perfusion image at rest shows that defect is reversible. *C*, SPECT images demonstrate normal myocardial perfusion with subdiaphragmatic attenuation artifact. *D*, Image from invasive coronary angiography demonstrates 85% stenosis in proximal left anterior descending artery (arrow).

higher than that for SPECT myocardial perfusion imaging in the diagnosis of an anatomic stenosis of at least 50% as defined with invasive angiography. This was consistent with a higher sensitivity for CT perfusion imaging; however, specificity for SPECT was higher. Predictive values demonstrated no difference in PPV; however, the NPV was higher for CT perfusion imaging. The increased sensitivity of CT perfusion imaging appears to be explained in part by its ability to depict varying levels of disease, including left main and multivessel CAD, better than SPECT.

The diagnostic differences between CT perfusion imaging and SPECT may be explained by technical differences in image resolution and tracer attributes. Previous studies comparing SPECT to cardiovascular MR imaging demonstrated that previous subendocardial infarction may be missed with SPECT (17) attributed that difference to limits in spatial resolution (7). As a result of the submillimeter spatial resolution of CT, previous studies have demonstrated that reductions in subendocardial attenuation, relative to subepicardial attenuation, are highly sensitive for the diagnosis of myocardial ischemia (1,2,18). Furthermore, differences in spatial resolution may also have a role in the observation that more patients with left main and multivessel CAD are detected with CT perfusion imaging. Balanced or

Table 2

Diagnostic Performance of Myocardial CT Perfusion Imaging: Per-Patient Analysis

	All Patients (n = 381)			Pharmacologic Stress Only (n = 257)		
Parameter	CT Perfusion Imaging	SPECT	P Value	CT Perfusion Imaging	SPECT	P Value
A_z	0.78 (74, 82)	0.69 (64, 74)	.001	0.78 (73, 83)	0.72 (66, 78)	.08
Sensitivity (%)	88 (83, 92) [202/229]	62 (56, 69) [143/229]	<.001	88 (82, 92) [142/162]	67 (59, 74) [109/162]	<.001
Specificity (%)	55 (46, 63) [83/152]	67(59, 75) [102/152]	.02	54 (43, 64) [51/95]	67 (57, 77) [64/95]	.06
PPV (%)	75 (69, 80) [202/271]	74 (67, 80) [142/193]	.87	76 (70, 82) [142/186]	78 (70, 84) [109/140]	.64
NPV (%)	75 (66, 83) [83/110]	54 (47, 62) [102/188]	<.001	72 (60, 82) [51/71]	55 (45, 64) [64/117]	.003

Note.—Numbers in parentheses are 95% CIs. Numbers in brackets are raw data.

Table 3

Diagnostic Performance of Myocardial CT Perfusion Imaging: Per-Vessel Analysis

Vessel and Modality	A_z	Sensitivity (%)	Specificity (%)	PPV (%)	NPV (%)
All vessels (n = 1143)					
CT perfusion imaging	0.74 (71, 78)	78 (73, 82) [356/459]	62 (58, 67) [427/684]	58 (53, 63) [356/613]	81 (76, 85) [427/530]
SPECT	0.69 (66, 72)	54 (48, 60) [249/459]	81 (77, 84) [551/684]	65 (59, 71) [249/382]	72 (68, 76) [551/761]
LAD (n = 381)					
CT perfusion imaging	0.75 (70, 79)	83(77, 89) [145/174]	55 (48, 62) [114/207]	61 (54, 67) [145/238]	80 (72, 86) [114/143]
SPECT	0.68 (63, 73)	47 (40, 55) [82/174]	86 (81, 90) [178/207]	74 (65, 82) [82/111]	66 (60, 72) [178/270]
LCX (n = 381)					
CT perfusion imaging	0.76 (71, 80)	82 (75, 88) [118/144]	56 (49, 62) [132/237]	53 (46, 60) [118/223]	84 (77, 89) [132/158]
SPECT	0.70 (65, 71)	60 (51, 68) [86/144]	74 (68, 80) [176/237]	59 (50, 67) [86/147]	75 (69, 81) [176/234]
RCA (n = 381)					
CT perfusion imaging	0.73 (68, 78)	66 (58, 74) [93/141]	75 (69, 81) [181/240]	61 (53, 69) [93/152]	79 (73, 84) [181/229]
SPECT	0.71 (66, 75)	57 (49, 66) [81/141]	82 (77, 87) [197/240]	65 (56, 74) [81/124]	77 (71, 82) [197/257]

Note.—Numbers in parentheses are 95% CIs. Numbers in brackets are raw data. For differences in A_z, P = .008 for all vessels, P = .02 for left anterior descending artery, P = .05 for left circumflex artery, and P = 043 for right coronary artery. LAD = left anterior descending artery, LCX = left circumflex artery, RCA = right coronary artery.

Table 4

Sensitivity of CT Perfusion Imaging and SPECT for Left Main, Three-Vessel, Two-Vessel, and One-Vessel Disease

Disease Type	CT Perfusion Imaging	SPECT
Left main	92 (62–100) [11/12]	75 (43–95) [9/12]
Three vessel	92 (83–97) [61/66]	79 (67–88) [52/66]
Two vessel	89 (80–95) [67/75]	68 (56–78) [51/75]
One vessel	83 (73–91) [63/76]	41 (30–53) [31/76]

Note.—Data are percentages. Numbers in parentheses are 95% CIs. Numbers in brackets are raw data.

more subtle subendocardial ischemia may be seen at CT but may not be appreciated at SPECT (19,20).

It is well known that decreases in myocardial blood flow begin when vessel diameter is reduced by at least 50% (9,10). However, the ability to detect small decreases in myocardial blood flow is dependent on the extraction fraction of a tracer. Technetium-based tracers are susceptible to the roll-off phenomenon, which limits the ability to differentiate differences in flow at higher levels owing to its limited extraction fraction (21). This typically affects the diagnosis of stenoses of 50%–70% but is less likely to affect the detection of stenoses of more than 70%. Conversely, iodinated contrast material has more favorable extraction characteristics, allowing for a linear relationship between CT-derived metrics and myocardial blood flow (22,23). This may explain why, in the primary analysis, the A_z of CT perfusion imaging for the detection of stenoses of at least 50% was higher than that of SPECT; however, this finding lost statistical significance at a threshold of at least 70% at posthoc analysis.

Another source of decreased sensitivity for SPECT may come from the fact that a large number of patients were on antianginal drugs such as β-blockers (45%) and nitrates (12%). β-blockers can decrease the size and severity of perfusion deficits (24), and,

in general, antianginal drugs reduce ischemic burden at SPECT (25). Sharir et al (25) previously demonstrated that antianginal drugs reduce myocardial ischemia most effectively in the territory of the left anterior descending and left circumflex arteries, with no significant reduction in the territory of the right coronary artery. Similarly, our study demonstrated higher sensitivity for CT perfusion imaging compared with SPECT in the left anterior descending and left circumflex territories, but not in the right coronary artery territory. These findings, along with the fact that 84% of our participants received β-blockers before CT, suggest that CT perfusion imaging is less susceptible to the effects of antianginal medications. This is of great benefit to protocols that begin with coronary CT angiography and are followed by CT perfusion imaging, allowing for low heart rates at rest and resulting in improved image quality and lower radiation dose.

Despite the rigorous prospective, multicenter design of CORE320, there are several limitations of the study that should be discussed. First, SPECT studies in CORE320, although obtained at validated laboratories, did not use attenuation correction. Attenuation correction has been shown to improve specificity, but is not yet in widespread use (26). Although this is a limitation, our study reflects contemporary clinical SPECT standards throughout four continents and eight nations and highlights the importance of attenuation correction. Second, SPECT and CT perfusion imaging are functional tools that measure tissue perfusion, reflecting the contribution of blood flow of all vessels, including collateral vessels, to a given area rather than delineating anatomic stenosis. In the case of sufficient perfusion due to collateral circulation, perfusion images may appear normal in downstream tissue despite an anatomic stenosis of at least 50%, resulting in a perceived decrease in sensitivity for detecting a stenosis. These pathophysiologic basics underlying perfusion imaging indicate that the use of a pure anatomic marker such as stenosis of at least 50% is a limited reference standard for assessing the clinical value of perfusion imaging. Furthermore, a normal SPECT study is indicative of good prognosis with respect to major cardiac events (27,28), which remains to be seen with regard to CT perfusion imaging. In addition, there are several limitations with regard to CT perfusion imaging and analysis in this study. In this study, we used a snapshot of myocardial perfusion distribution during the upslope to peak of the contrast material infusion acquired over one to two heart beats. This is much different from dynamic CT perfusion imaging, which provides serial images of myocardial perfusion and can quantify myocardial blood flow in absolute terms (22,23,29). Furthermore, in this study we examined the diagnostic performance of CT perfusion imaging alone in the detection of anatomic stenosis. In clinical practice, CT perfusion imaging will mostly be used in conjunction with CT angiography. Previous studies have demonstrated that CT perfusion imaging, when added to CT angiography, improves the diagnostic accuracy of CT angiography in the prediction of anatomic stenosis (30,31). In this study, we made our best attempt to blind the reader of the CT perfusion images to the coronary CT angiograms by fixing the window width and level and section thickness, making the interpretation of percentage stenosis very difficult. However, it is possible that calcified plaque could be seen with these settings and may have biased the CT perfusion reader toward higher sensitivity for anatomic stenosis. Last, the lower specificity for CT perfusion imaging demonstrated in this study may be due to a number of factors. Although we used a myocardial-specific beam-hardening correction (32), residual beam-hardening artifacts may have contributed to false-positive CT perfusion studies. In addition, adenosine increased the median heart rate to 69 beats per minute (interquartile range, 60–78 beats per minute), potentially increasing motion artifacts that may be mistaken for perfusion abnormalities. Recognizing these issues, we prespecified a SSS threshold of at least 2 for CT perfusion imaging to account for potential artifacts.

The primary aim of the CORE320 study was to diagnose an angiographic stenosis causing a myocardial perfusion deficit by using a combination of coronary CT angiography and myocardial CT perfusion imaging and compare findings with those of the combined standard of reference of coronary angiography and SPECT. Although the combination of coronary angiography and SPECT is a rigorous standard of reference for defining hemodynamically significant stenosis and is used daily in clinical practice, this study and others demonstrated that SPECT can be limited in the setting of left main and multivessel CAD (19,20). Because a normal SPECT study in the setting of left main and multivessel disease would have made the reference standard normal, this may have had a substantial effect on the measured specificity and PPV of combined CT angiography and CT perfusion imaging in the primary CORE320 study (5).

In conclusion, in this prospective, multicenter study, myocardial CT perfusion imaging demonstrated higher overall diagnostic performance, as demonstrated with the A_z, compared with SPECT for the diagnosis of anatomic stenosis of at least 50%. CT perfusion imaging demonstrated higher sensitivity, whereas SPECT demonstrated higher specificity. The higher sensitivity of CT perfusion imaging is driven in part by its higher sensitivity in the detection of left main and multivessel CAD.

Disclosures of Conflicts of Interest: R.T.G. Financial activities related to the present article: institution received a grant from Toshiba Medical Systems; received grants from Toshiba and GE Healthcare; is a paid consultant for ICON Medical Imaging. Financial activities not related to the present article: none to disclose. Other relationships: has patents issued. **V.C.M.** Financial activities related to the present article: institution received a grant from Toshiba Medical Systems. Financial activities not related to the present article: none to disclose. Other relationships: none to disclose. **M.Y.C.** No relevant conflicts of interest to disclose. **K.K.** Financial activities related to the present article: institution received a grant from Toshiba Medical Systems. Financial activities not related to the present article: institution has grants/grants pending from Siemens and Bayer; receives payment for

lectures including service on speakers bureaus from Siemens. Other relationships: none to disclose. **A.A.** Financial activities related to the present article: institution received a grant from Toshiba Medical Systems; institution receives support for travel to meetings for study or other purposes from Toshiba Medical Systems. Financial activities not related to the present article: none to disclose. Other relationships: none to disclose. **J.M.M.** Financial activities related to the present article: institution received a grant from Toshiba Medical Systems. Financial activities not related to the present article: received a grant through the university for study services. Other relationships: none to disclose. **M.B.M.** Financial activities related to the present article: institution received a grant from Toshiba Medical Systems. Financial activities not related to the present article: none to disclose. Other relationships: none to disclose. **A.L.V.** Financial activities related to the present article: institution received a grant from Toshiba Medical Systems. Financial activities not related to the present article: none to disclose. Other relationships: none to disclose. **K.F.K.** Financial activities related to the present article: institution received a grant from Toshiba Medical Systems; institution received support for travel to meetings for the study or other purposes from Toshiba Medical Systems. Financial activities not related to the present article: none to disclose. Other relationships: none to disclose. **C.E.R.** Financial activities related to the present article: received support for travel to meetings for the study or other purposes from Toshiba Medical Systems. Financial activities not related to the present article: none to disclose. Other relationships: none to disclose. **M.D.** Financial activities related to the present article: institution received a grant from Toshiba Medical Systems. Financial activities not related to the present article: is a paid consultant for Guerbet; institution has grants/grants pending from GE Healthcare, Bracco, Guerbet, and Toshiba Medical Systems; receives payment for development of educational presentations including service on speakers bureaus from Toshiba Medical Systems, Bayer-Schering, and Guerbet; institution receives travel/accommodations expenses from Toshiba Medical Systems and Guerbet; receives royalties from Springer. Other relationships: none to disclose. **T.S.Y.** Financial activities related to the present article: institution received a grant from Toshiba Medical Systems; receives payment for service on speakers bureau from Toshiba Medical Systems none to disclose. Financial activities not related to the present article: none to disclose. Other relationships: none to disclose. **H.N.** Financial activities related to the present article: institution received a grant from Toshiba Medical Systems. Financial activities not related to the present article: none to disclose. Other relationships: none to disclose. **W.B.** Financial activities related to the present article: none to disclose. Financial activities not related to the present article: is on the advisory board for Bayer. Other relationships: none to disclose. **C.C.** Financial activities related to the present article: institution received a grant from Toshiba Medical Systems. Financial activities not related to the present article: none to disclose. Other relationships: none to disclose. **M.E.C.** No relevant conflicts of interest to disclose. **J.A.C.L.** Financial activities related to the present article: institution received a grant from Toshiba Medical Systems. Financial activities not related to the present article: none to disclose. Other relationships: none to disclose. **M.D.C.** Financial activities related to the present article: institution received a grant from Toshiba Medical Systems; institution received support for travel to meetings for the study or other purposes from Toshiba Medical Systems. Financial activities not related to the present article: none to disclose. Other relationships: none to disclose.

References

1. George RT, Arbab-Zadeh A, Miller JM, et al. Adenosine stress 64- and 256-row detector computed tomography angiography and perfusion imaging: a pilot study evaluating the transmural extent of perfusion abnormalities to predict atherosclerosis causing myocardial ischemia. Circ Cardiovasc Imaging 2009;2(3):174–182.
2. George RT, Arbab-Zadeh A, Miller JM, et al. Computed tomography myocardial perfusion imaging with 320-row detector computed tomography accurately detects myocardial ischemia in patients with obstructive coronary artery disease. Circ Cardiovasc Imaging 2012;5(3):333–340.
3. Blankstein R, Shturman LD, Rogers IS, et al. Adenosine-induced stress myocardial perfusion imaging using dual-source cardiac computed tomography. J Am Coll Cardiol 2009;54(12):1072–1084.
4. Bettencourt N, Chiribiri A, Schuster A, et al. Direct comparison of cardiac magnetic resonance and multidetector computed tomography stress-rest perfusion imaging for detection of coronary artery disease. J Am Coll Cardiol 2013;61(10):1099–1107.
5. Rochitte CE, George RT, Chen MY, et al. Computed tomography angiography and perfusion to assess coronary artery stenosis causing perfusion defects by single photon emission computed tomography: the CORE320 study. Eur Heart J 2014;35(17):1120–1130.
6. San Román JA, Vilacosta I, Castillo JA, et al. Selection of the optimal stress test for the diagnosis of coronary artery disease. Heart 1998;80(4):370–376.
7. Greenwood JP, Maredia N, Younger JF, et al. Cardiovascular magnetic resonance and single-photon emission computed tomography for diagnosis of coronary heart disease (CE-MARC): a prospective trial. Lancet 2012;379(9814):453–460.
8. Miller JM, Rochitte CE, Dewey M, et al. Diagnostic performance of coronary angiography by 64-row CT. N Engl J Med 2008;359(22):2324–2336.
9. Uren NG, Melin JA, De Bruyne B, Wijns W, Baudhuin T, Camici PG. Relation between myocardial blood flow and the severity of coronary-artery stenosis. N Engl J Med 1994;330(25):1782–1788.
10. Di Carli M, Czernin J, Hoh CK, et al. Relation among stenosis severity, myocardial blood flow, and flow reserve in patients with coronary artery disease. Circulation 1995;91(7):1944–1951.
11. Gottsauner-Wolf M, Sochor H, Moertl D, Gwechenberger M, Stockenhuber F, Probst P. Assessing coronary stenosis: quantitative coronary angiography versus visual estimation from cine-film or pharmacological stress perfusion images. Eur Heart J 1996;17(8):1167–1174.
12. George RT, Arbab-Zadeh A, Cerci RJ, et al. Diagnostic performance of combined noninvasive coronary angiography and myocardial perfusion imaging using 320-MDCT: the CT angiography and perfusion methods of the CORE320 multicenter multinational diagnostic study. AJR Am J Roentgenol 2011;197(4):829–837.
13. Vavere AL, Simon GG, George RT, et al. Diagnostic performance of combined noninvasive coronary angiography and myocardial perfusion imaging using 320 row detector computed tomography: design and implementation of the CORE320 multicenter, multinational diagnostic study. J Cardiovasc Comput Tomogr 2011;5(6):370–381.
14. Cerci RJ, Arbab-Zadeh A, George RT, et al. Aligning coronary anatomy and myocardial perfusion territories: an algorithm for the CORE320 multicenter study. Circ Cardiovasc Imaging 2012;5(5):587–595.
15. Henzlova MJ, Cerqueira MD, Hansen CL, Taillefer R, Yao SS. ASNC imaging guidelines for nuclear cardiology procedures: stress protocols and tracers. J Nucl Cardiol 2009;16(2):331.
16. Miller JM, Dewey M, Vavere AL, et al. Coronary CT angiography using 64 detector rows: methods and design of the multi-centre trial CORE-64. Eur Radiol 2009;19(4):816–828.
17. Wagner A, Mahrholdt H, Holly TA, et al. Contrast-enhanced MRI and routine single photon emission computed tomography (SPECT) perfusion imaging for detection of subendocardial myocardial infarcts: an imaging study. Lancet 2003;361(9355):374–379.
18. Ko BS, Cameron JD, Leung M, et al. Combined CT coronary angiography and stress myocardial perfusion imaging for hemodynamically significant stenoses in patients

with suspected coronary artery disease: a comparison with fractional flow reserve. JACC Cardiovasc Imaging 2012;5(11):1097–1111.

19. Berman DS, Kang X, Slomka PJ, et al. Underestimation of extent of ischemia by gated SPECT myocardial perfusion imaging in patients with left main coronary artery disease. J Nucl Cardiol 2007;14(4):521–528.
20. Svane B, Bone D, Holmgren A. Coronary angiography and thallium-201 single photon emission computed tomography in multiple vessel coronary artery disease. Acta Radiol 1990;31(4):325–332.
21. Dilsizian V. SPECT and PET myocardial perfusion imaging: tracers and techniques. In: Dilsizian V, Narula J, eds. Atlas of nuclear cardiology. 4th ed. New York, NY: Springer, 2013; 55–94.
22. Ichihara T, George RT, Silva C, Lima JA, Lardo AC. Quantitative analysis of first-pass contrast-enhanced myocardial perfusion multidetector CT using a Patlak plot method and extraction fraction correction during adenosine stress. IEEE Trans Nucl Sci 2011;58(1):133–138.
23. George RT, Jerosch-Herold M, Silva C, et al. Quantification of myocardial perfusion using dynamic 64-detector computed tomography. Invest Radiol 2007;42(12):815–822.
24. Böttcher M, Czernin J, Sun K, Phelps ME, Schelbert HR. Effect of beta 1 adrenergic receptor blockade on myocardial blood flow and vasodilatory capacity. J Nucl Med 1997;38(3):442–446.
25. Sharir T, Rabinowitz B, Livschitz S, et al. Underestimation of extent and severity of coronary artery disease by dipyridamole stress thallium-201 single-photon emission computed tomographic myocardial perfusion imaging in patients taking antianginal drugs. J Am Coll Cardiol 1998;31(7):1540–1546.
26. Venero CV, Heller GV, Bateman TM, et al. A multicenter evaluation of a new post-processing method with depth-dependent collimator resolution applied to full-time and half-time acquisitions without and with simultaneously acquired attenuation correction. J Nucl Cardiol 2009;16(5):714–725.
27. Iskander S, Iskandrian AE. Risk assessment using single-photon emission computed tomographic technetium-99m sestamibi imaging. J Am Coll Cardiol 1998;32(1):57–62.
28. Hachamovitch R, Berman DS, Shaw LJ, et al. Incremental prognostic value of myocardial perfusion single photon emission computed tomography for the prediction of cardiac death: differential stratification for risk of cardiac death and myocardial infarction. Circulation 1998;97(6):535–543.
29. Bamberg F, Becker A, Schwarz F, et al. Detection of hemodynamically significant coronary artery stenosis: incremental diagnostic value of dynamic CT-based myocardial perfusion imaging. Radiology 2011;260(3):689–698.
30. Rocha-Filho JA, Blankstein R, Shturman LD, et al. Incremental value of adenosine-induced stress myocardial perfusion imaging with dual-source CT at cardiac CT angiography. Radiology 2010;254(2):410–419.
31. Rief M, Zimmermann E, Stenzel F, et al. Computed tomography angiography and myocardial computed tomography perfusion in patients with coronary stents: prospective intraindividual comparison with conventional coronary angiography. J Am Coll Cardiol 2013;62(16):1476–1485.
32. Kitagawa K, George RT, Arbab-Zadeh A, Lima JA, Lardo AC. Characterization and correction of beam-hardening artifacts during dynamic volume CT assessment of myocardial perfusion. Radiology 2010;256(1):111–118.